Bioorganic & Medicinal Chemistry Letters 23 (2013) 6097–6105

Contents lists available at ScienceDirect

Bioorganic & Medicinal Chemistry Letters

journal homepage: www.elsevier.com/locate/bmcl

Rational drug design based synthesis of novel arylquinolines as anti-tuberculosis agents

Puneet P. Jain [a], Mariam S. Degani [a,*], Archana Raju [a], Muktikanta Ray [b], M. G. R. Rajan [b]

[a] Institute of Chemical Technology, Nathalal Parekh Marg, Matunga, Mumbai 400019, India
[b] Radiation Medicine Centre, Tata Memorial Hospital, Parel, Mumbai, India

ARTICLE INFO

Article history:
Received 24 July 2013
Revised 5 September 2013
Accepted 7 September 2013
Available online 16 September 2013

Keywords:
Mycobacterium tuberculosis
ATP synthase
Bedaquiline
Arylquinoline

ABSTRACT

A series of novel arylquinoline derivatives was designed retaining significant pharmacophoric features and three dimensional geometry of bedaquiline. In silico ADME study was performed to assess drug likeness and toxicity profiles of the designed molecules. The compounds were evaluated for activity against *Mycobacterium tuberculosis* $H_{37}Rv$ using Resazurin Microtitre Assay (REMA) plate method and cytotoxicity in VERO C1008 cell line. Several of the synthesized compounds exhibited good antituberculosis activity and selectivity, especially compounds, **12i** (MIC: 5.18 μM and MIC/CC_{50}: 152.86) and **12l** (MIC: 5.59 μM and MIC/CC_{50}: 160.57). The study opens up a new platform for the development of arylquinoline based drugs for treating tuberculosis.

Tuberculosis (TB), caused by *Mycobacterium tuberculosis* (*Mtb*) is one of the primary health threats to mankind. It is the greatest cause of mortality worldwide amongst infectious diseases, with approximately 1.4 million reported deaths in 2011.[1] The existence and rise of drug resistant strains and the recent emergence of new forms of Extensively Drug Resistant TB (XDR-TB)[1,2] have raised serious questions about the effectiveness of the existing therapy. The challenge of combating this severe and deadly form of TB requires significant efforts towards discovery of novel anti-TB agents.

Quinoline-based compounds are known to display a wide variety of important pharmacological activities including tuberculosis.[3,4] Recently, a new class of quinoline based anti-TB agents, diarylquinolines (DARQ's), are proven to act by a novel mechanism of action. They act by binding to F_0 intra-membrane portion of *Mycobacterium tuberculosis* adenosine triphosphate synthase (*Mtb*ATPase) and interfere with the normal production of ATP. Bedaquiline (Fig. 1), the lead compound of the DARQ series, displays MIC of 0.06 μg/mL (i.e. 0.108 μM) against *M. tuberculosis* $H_{37}Rv$. It is equally active against a variety of antibiotic-susceptible strains as well as strains resistant to drugs like isoniazid, rifampin, streptomycin, ethambutol, pyrazinamide, and moxifloxacin.[5,6] It also shows a selectivity of > 20,000:1 towards mycobacterial ATP synthase as compared to human mitochondrial ATP synthase.[7] Bedaquiline was recently approved for use by the U.S. Food and Drug Administration (FDA) against Multi-drug resistant TB (MDR-TB).[8] Thus, its scaffold is interesting for further exploration to find novel molecules against TB.

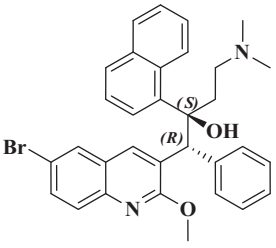

Figure 1. Bedaquiline.

Our design strategy was aimed at developing potent molecules, with crucial pharmacophoric features and a three dimensional geometry similar to bedaquiline. The approach used complies with the fact that a receptor can perceive the shape and electrostatic properties of a molecule that binds to it.[9] So, if a new compound matches the shape and electrostatic properties of a known molecule, then it is likely to bind as well. Consequently, an in silico binding interaction study of bedaquiline using the homology model of *Mtb*ATPase, was carried out to understand the key residues involved in the binding of bedaquiline and functioning of *Mtb*ATPase. Based on the pharmacophoric features of bedaquiline and in silico druggability evaluation, we herein report the design and synthesis

* Corresponding author. Tel.: +91 22 3361 2213; fax: +91 22 3361 1020.
E-mail addresses: ms.degani@ictmumbai.edu.in, m_degani@yahoo.co (M.S. Degani).

0960-894X/$ - see front matter © 2013 Elsevier Ltd. All rights reserved.
http://dx.doi.org/10.1016/j.bmcl.2013.09.027

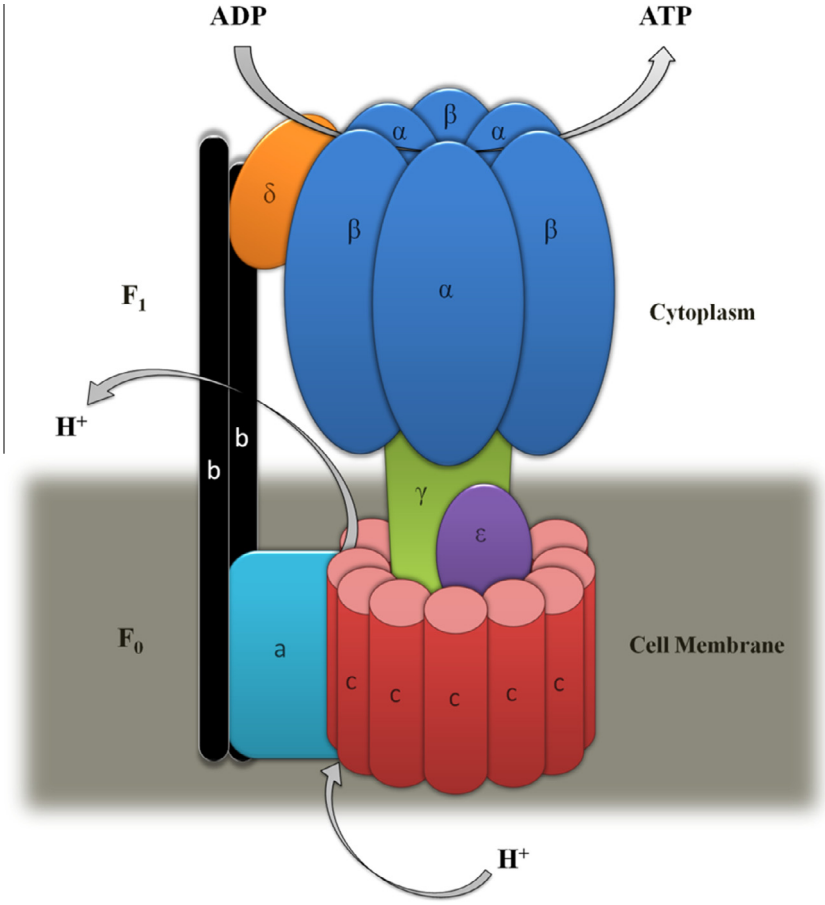

Figure 2. F_1F_0 ATP synthase.

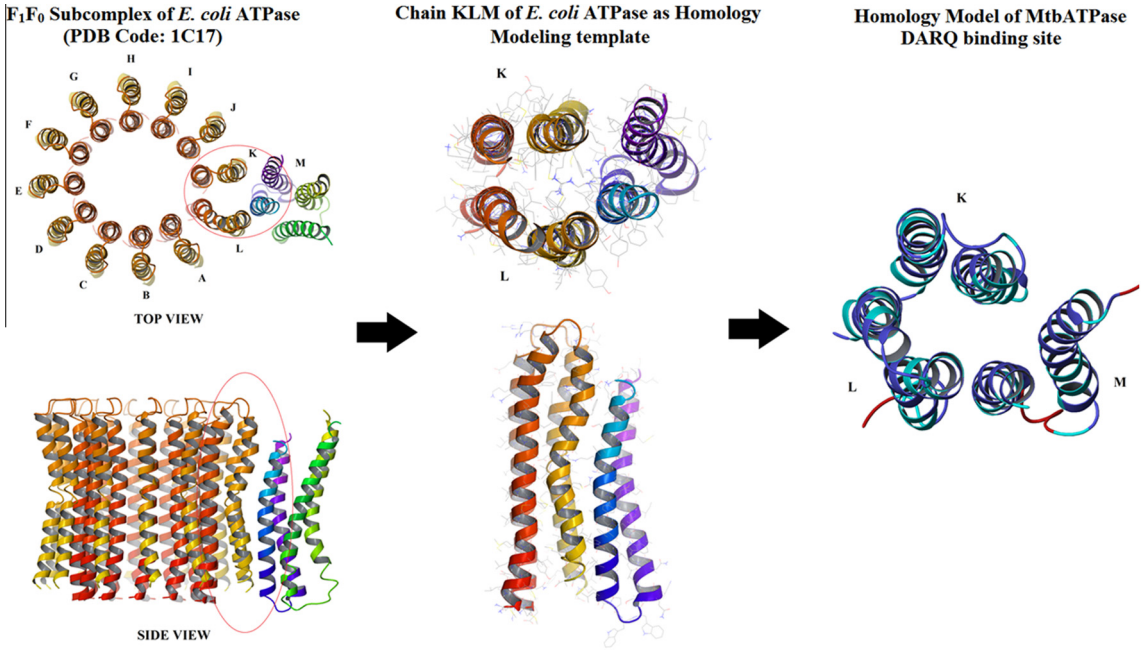

Figure 3. Homology modeling of DARQ binding site.

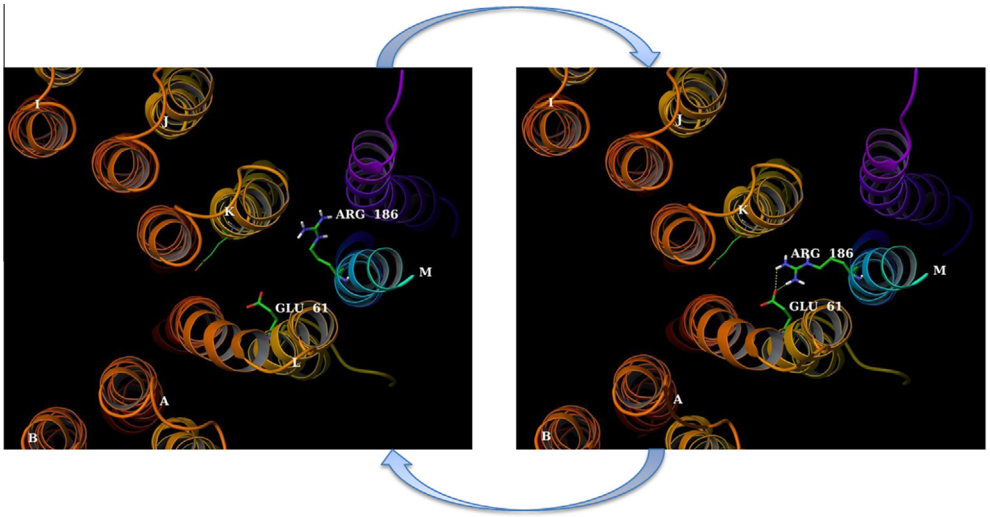

Figure 4. Molecular mechanism of *Mtb*ATPase.

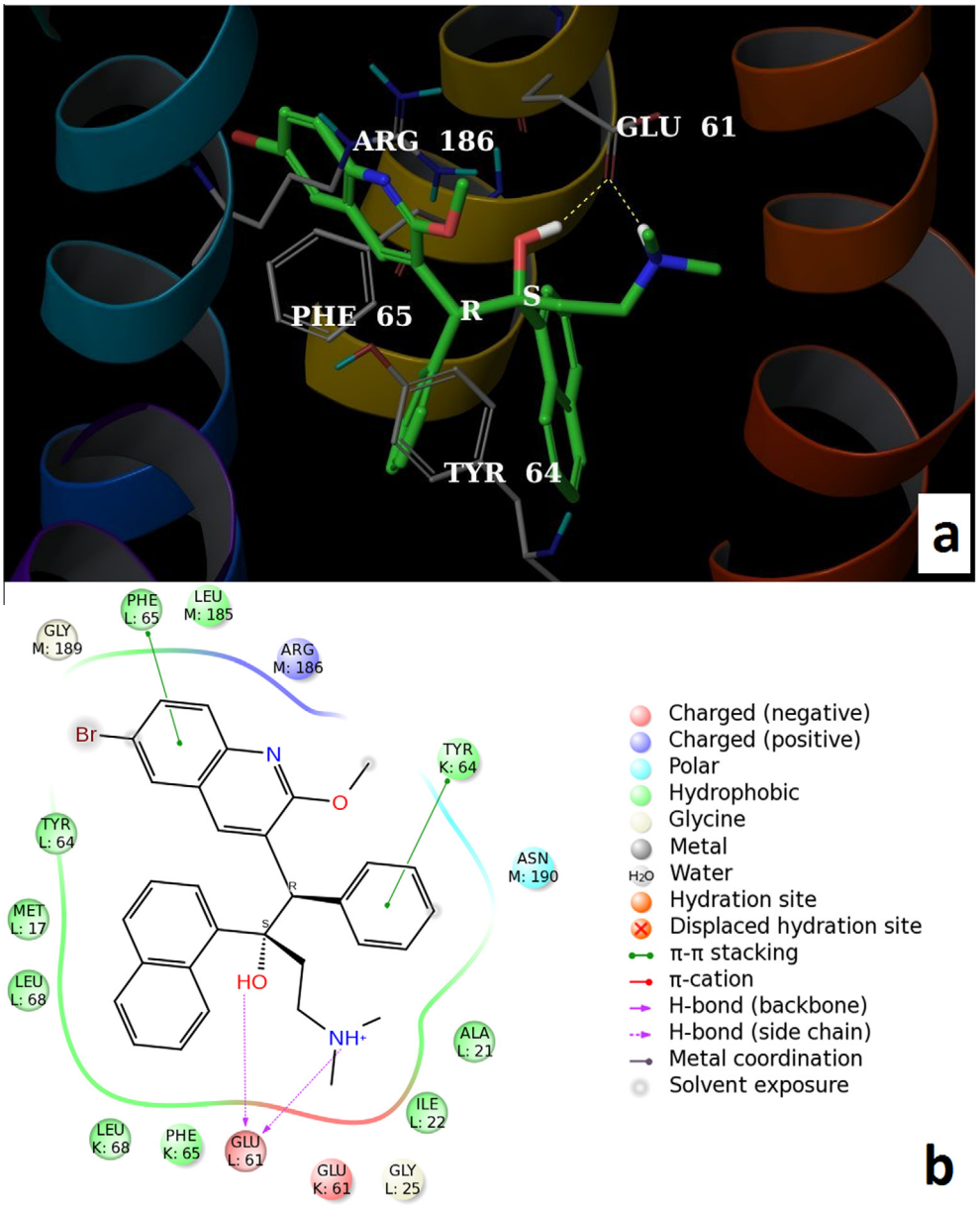

Figure 5. (a) Docking interaction of bedaquiline at DARQ binding site of *Mtb*ATPase; (b) ligand interaction diagram of bedaquiline.

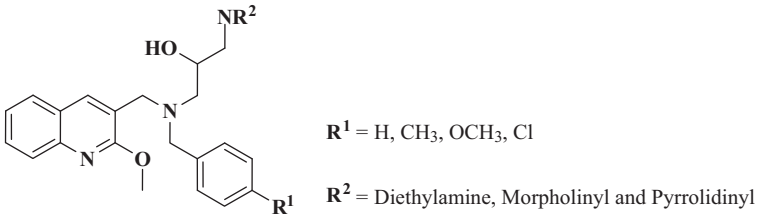

Figure 6. Novel arylquinoline scaffold.

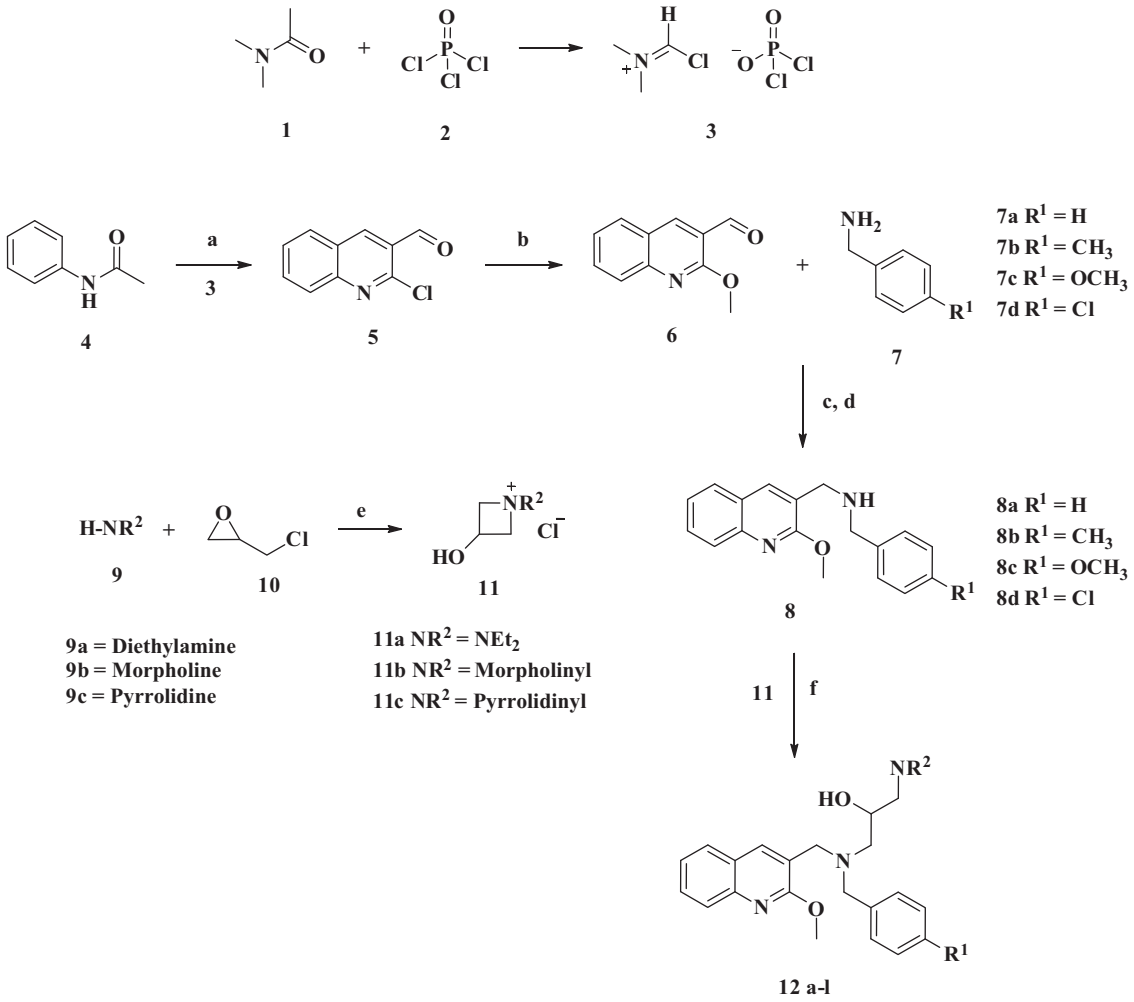

Scheme 1. Synthetic route for the synthesis of arylquinoline derivatives (**12a–l**). Reagents and conditions: (a) DMF–$POCl_3$ Vilsmeier–Haack reagent (3), 80 °C, 16.5 h; (b) MeOH, KOH, reflux, 3–4 h; (c) EtOH, cat. AcOH, reflux, 12 h; (d) EtOH, sodium borohydride, rt, 6 h; (e) EtOH, reflux; (f) 3-hydroxyazetidinium chloride (**11a–c**), EtOH, relux.

of a series of novel arylquinoline derivatives (Fig. 6) with promising anti-TB activity against *Mycobacterium tuberculosis* $H_{37}Rv$.

A typical F_1F_0 ATPase enzyme consists of two structural domains: F_0, a hydrophobic intramembraneous proton channel, composed of $a_1b_2c_{10-15}$ subunits and F_1, a hydrophilic extramembraneous catalytic core, composed of $\alpha_3\beta_3\gamma\delta\varepsilon$ subunits that extend into cytoplasm. Both F_1 and F_0 are linked together by a central and a peripheral stalk (Fig. 2). During catalysis, translocation of proton through F_0 triggers rotation of the oligomeric subunit-c ring, which is coupled via central stalk subunits to the rotary mechanism of the $(\alpha\beta)_3$ hexamer of the catalytic domain, F_1 which finally drives the synthesis of ATP from ADP.[10–14]

In *Mtb*ATPase, DARQ binding site is located at the junction of subunit-a and subunit-c. As it is very difficult to crystallize membrane bound proteins such as ATPases, no crystal structure of *Mtb*ATPase is currently available. As an alternative, a homology model of DARQ binding site was generated using NMR solution structure of F_0-region of *Escherichia coli* ATPase (PDB code: 1C17)[14] as the template. The homology modeling was performed with the help of inputs from earlier literature,[15] using Prime module of Maestro,[16] a molecular modeling suite. The homology model thus generated was made up of two c-subunits (2-helices of chain K & L each) and one a-subunit (2-helices of chain M) (Fig. 3).

Table 1
The shape similarity scores with respect to bedaquiline and des-phenyl bedaquiline

Compounds	R^1	NR^2	Shape_sim score	
			Bedaquiline	Des-phenyl bedaquiline
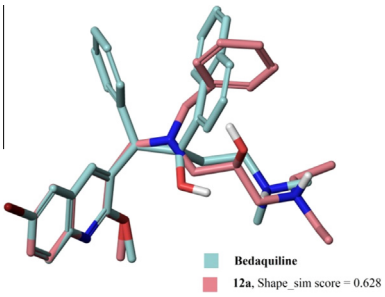			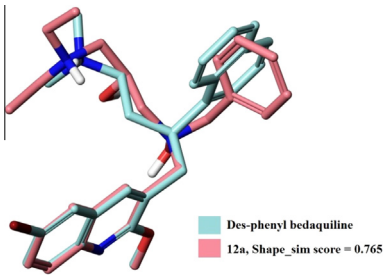	
12a	H	$N(C_2H_5)_2$	0.628	0.765
12b	CH_3	$N(C_2H_5)_2$	0.637	0.789
12c	OCH_3	$N(C_2H_5)_2$	0.641	0.771
12d	Cl	$N(C_2H_5)_2$	0.640	0.759
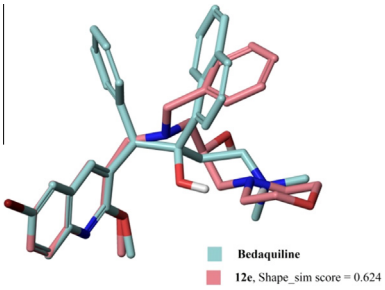			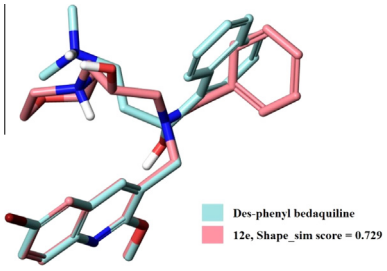	
12e	H	Morpholinyl	0.624	0.729
12f	CH_3	Morpholinyl	0.631	0.744
12g	OCH_3	Morpholinyl	0.618	0.717
12h	Cl	Morpholinyl	0.634	0.698
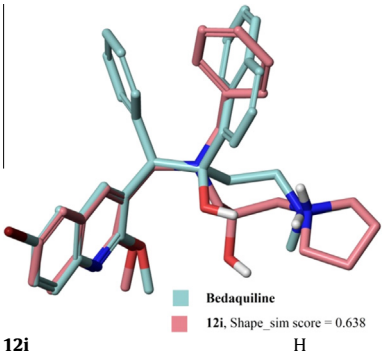			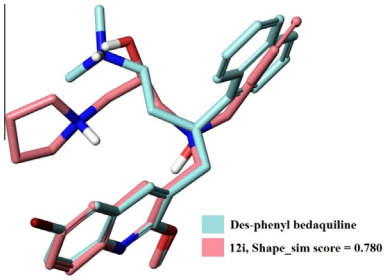	
12i	H	Pyrrolidinyl	0.638	0.780
12j	CH_3	Pyrrolidinyl	0.621	0.761
12k	OCH_3	Pyrrolidinyl	0.642	0.788
12l	Cl	Pyrrolidinyl	0.623	0.765

Table 2
Qikprop analysis results of designed aryl quinoline derivatives along with that of bedaquiline

Compound	MW[a]	#Stars[b]	CNS[c]	QPlogPo/w[d]	QPPCaco[e]	% HOA[f]	Rule of five[g]
Bedaquiline	555.51	4	1	7.633	1683.293	100	2
12a	407.56	0	1	4.143	407.601	100	0
12b	421.59	0	1	4.524	346.949	100	0
12c	437.58	0	1	4.191	329.885	96.56	0
12d	442.00	0	1	4.961	397.672	100	0
12e	421.54	0	2	3.241	361.262	91.08	0
12f	435.57	0	2	3.426	322.109	91.85	0
12g	451.57	0	1	3.429	347.305	91.43	0
12h	455.98	0	2	3.611	406.118	94.44	0
12i	405.54	0	1	3.881	296.957	93.61	0

(*continued on next page*)

Table 2 (*continued*)

Compound	MW[a]	#Stars[b]	CNS[c]	QPlogPo/w[d]	QPPCaco[e]	% HOA[f]	Rule of five[g]
12j	419.57	0	1	4.118	289.675	95.00	0
12k	435.57	0	1	3.849	349.254	95.00	0
12l	439.98	0	2	4.181	254.825	94.49	0

[a] Molecular weight—acceptable limit is <500 Da.
[b] #stars—this property indicates the number of property or descriptor values that fall outside the 95% range of similar values for known drugs. A large number of stars suggest that a molecule is less drug-like than molecules with few stars. The range predicted for this parameter using QikProp is 0–5; where 0 indicates no violation or best candidate.
[c] CNS—this exhibits the predicted central nervous system activity on a –2 (inactive) to +2 (active) scale.
[d] QP log Po/w—this gives the predicted octanol/water partition coefficient. The acceptable range predicted for this parameter using QikProp is −2.0 to 6.5.
[e] QPPcaco—this gives the predicted apparent Caco-2 cell permeability in nm/s. Caco-2 cells are a model for the gut–blood barrier. QikProp predictions are for non-active transport, where <25 is considered poor and >500 is considered excellent.
[f] Percentage human oral absorption—this gives the predicted human oral absorption on 0–100% scale. The prediction is based on a quantitative multiple linear regression model. Value of >80% is considered good and <25% is considered poor.
[g] Rule of five—this property denotes the number of violations of Lipinski's rule of five. The rules includes: MW < 500, QPlogPo/w < 5, donorHB ⩽ 5, accptHB ⩽ 10. Compounds that satisfy these rules are considered drug like.

Table 3
Arylquinoline derivatives with their antimycobacterial activity, cytotoxicity and dock score

Compounds	MIC[a] (μM)	CC_{50}[b] (μM)	SI	Dock score
12a	40.63	613.41	15.10	−7.225
12b	19.31	1008.09	52.21	−7.747
12c	79.12	726.72	9.19	−7.308
12d	10.05	807.69	80.41	−8.678
12e	97.10	552.74	5.69	−5.880
12f	21.88	883.90	40.40	−7.420
12g	158.34	927.87	5.86	−5.369
12h	20.20	1059.26	52.44	−6.794
12i	5.18	791.54	152.86	−7.551
12j	9.68	1113.04	115.02	−8.452
12k	18.64	663.50	35.59	−7.522
12l	5.59	897.77	160.57	−9.220
INH	15.3	1470	96	—

SI—Selective Index.
INH—Isoniazid.
[a] Compounds were tested against *Mtb* $H_{37}Rv$ strains using REMA method.
[b] Cytotoxicity studies were done on VERO cell line C1008 using MTT assay.

Arg-186 of the a-subunit and Glu-61 of the c-subunits are well known to play a crucial role in the rotary mechanism of the c-subunits. This rotary mechanism consists of a cycle, which is initiated with a conformational change of the folded form of non-ionized Arg-186 to the extended form of ionized Arg-186, on acceptance of proton from the proton transfer chain. Then a proton transfer from the extended Arg-186 to COO^- group of Glu-61 causes drastic conformational changes leading to a 30° rotation of the c-subunits. Lastly, the neutral form of Arg-186 reverts back to its initial folded form (Fig. 4). Bedaquiline acts by mimicking the extended charged form of Arg-186, thus interfering with its role and the rotary movement of c-subunits, blocking the proton transfer process and thereby ATPase activity.[15]

An in silico docking study of bedaquiline at the DARQ binding site was performed to identify the key residues involved in binding of bedaquiline (Fig. 5).

The mode of inhibition by bedaquiline and its docking interaction at the active binding site clearly explains the importance of protonated tertiary amino functionality that acts similar to M:Arg-186 by forming a H-bond with the L:Glu-61, a key towards its ATPase inhibitory activity. The π-π stacking interactions of quinoline ring with L:Phe-65 and phenyl ring with K:Tyr-64 are crucial for the stability of protein–ligand complex. H-bonding of the hydroxyl moiety with L:Glu-61 may add stability to the complex, but may or may not be crucial for the activity. Other features such as the naphthalene ring and bromo-substitution may enhance the penetration across the *Mycobacterial* cell wall by increasing the lipophilicity of bedaquiline.

Based on the essential pharmacophoric features of bedaquiline, a novel scaffold of arylquinoline derivatives were designed, retaining the 2-methoxyquinoline core. Benzyl functionality was added for π-π stacking interactions with the crucial residues, similar to phenyl functionality in bedaquiline. The 2-(dialkylamino)ethanol-1-yl functionality was added to mimic the indispensable L:Glu-61 interaction. Addition of a tertiary amino linker between the benzyl- and 2-(dialkylamino)ethanol-1-yl side chain gave the molecule a three dimensional geometry similar to bedaquiline. A series of twelve arylquinoline derivatives were designed using combinations of substitutions at two places, $\mathbf{R^1}$ and $\mathbf{NR^2}$ (Fig. 6). $\mathbf{R^1}$ substitutions were chosen to check the effect of electronic and hydrophobic parameters on the activity and $\mathbf{NR^2}$ substitutions for the effect of tertiary amine in the form of aliphatic and cyclic systems.

A shape-based superimposition and similarity screening of arylquinoline derivatives was performed using Phase Shape module[9] in Maestro.[16] In order to better reflect the similarity of these derivatives against the bedaquiline scaffold, a study was performed taking bedaquiline as well as des-phenyl bedaquiline as templates. Shape similarity scores are in the range of 0–1, where 1 indicates shape identical to template and 0 indicates a shape which does

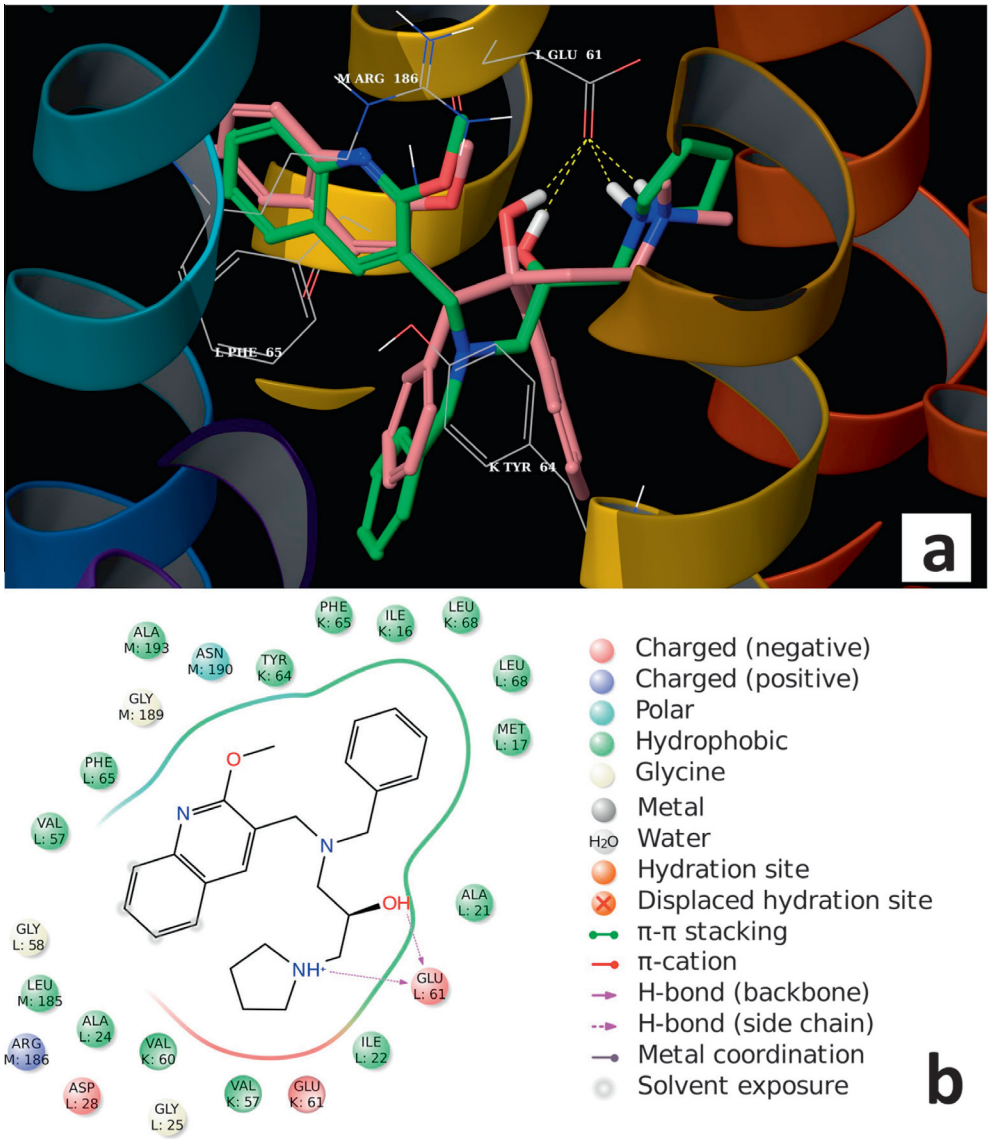

Figure 7. (a) Similar interaction of most active compound **12i** (Green) in comparison to bedaquiline (pink); (b) ligand interaction diagram of compound **12i**.

not match template at all.[9] The designed molecules show shape similarity scores ranging from 0.618 to 0.642 versus bedaquiline, and 0.698 to 0.789 versus des-phenyl bedaquiline, indicating three dimensional geometry reasonably similar to the bedaquiline scaffold (Table 1).

An in silico ADME prediction to check the druggability of the arylquinoline derivatives was performed using QikProp,[17] a program that predicts several significant physical descriptors and relevant pharmaceutical properties of organic molecules. It provides ranges for comparing the properties of a particular molecule with those of 95% of known drugs. The descriptors calculated were partition coefficient, Lipinski's rule of five, human oral absorption, CNS activity and gut-blood barrier permeability. All the arylquinoline derivatives passed the ADME check (Table 2), indicating that the designed molecules have drug-like properties.

The arylquinoline derivatives, i.e. **12a-l**, were synthesized according to Scheme 1 starting with Meth-Cohn quinoline synthesis reaction[18] of acetanilide (**4**) using Vilsmeier–Haack reagent (**3**) to form 2-chloro-3-formylquinoline (**5**). Compound **3** was generated in situ by reacting *N*,*N*-dimethylformamide (**1**) with excess of phosphorous oxychloride (**2**). Next, a 2-methoxy-3-formylquinoline (**6**) was synthesized by refluxing **5** in methanolic KOH solution. An indirect reductive amination method[19] was used to synthesize the secondary amine (**8**). The reaction involves in situ formation of a Schiff's base intermediate by refluxing **6** with relevant substituted benzylamines (**7a-d**) and subsequent borohydride reduction to obtain **8**. Alongside, a 3-hydroxyazetidinium chloride (**11a-c**) intermediate is synthesized by refluxing epichlorhydrin (**10**) with different starting secondary amines (**9**).[20] Finally, the arylquinoline derivatives (**12a-l**) were synthesized by azetidinol ring opening reaction,[21] by refluxing **8** with corresponding intermediate **11**.

All the synthesized compounds, **12a-l** were screened against *Mtb* $H_{37}Rv$ using a twofold dilution technique, in order to determine the minimum inhibitory concentration (MIC) using Resazurin Microtitre Assay (REMA) plate method.[22] The MIC was determined by visual inspection (color of dye changes from blue to pink in case of growth). Isoniazid (INH) was used as the standard drug. The compounds were also evaluated for toxicity on mammalian VERO

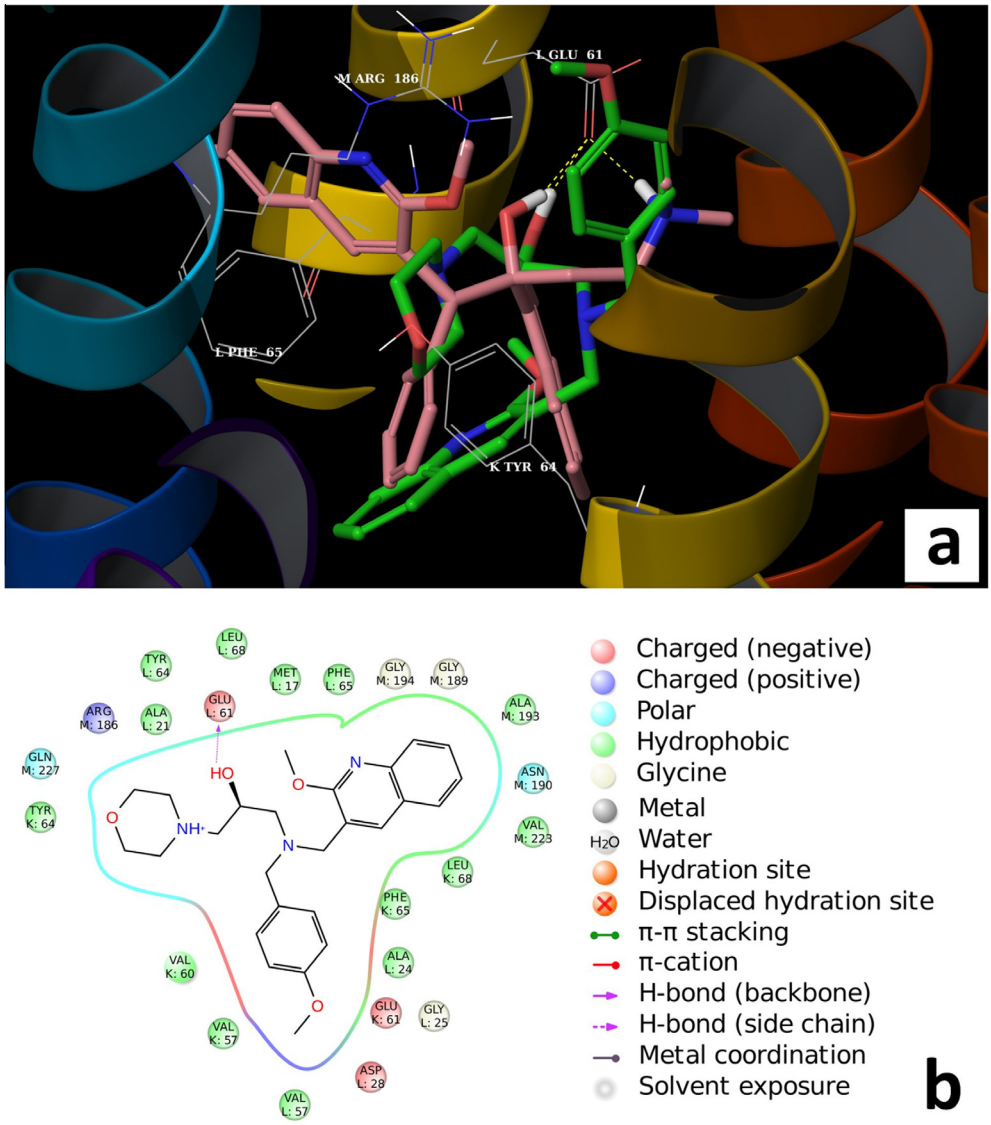

Figure 8. (a) Dissimilar interaction of least active compound **12g** (Green) in comparison to bedaquiline (pink); (b) ligand interaction diagram of compound **12g**.

cell line (C1008) using 96-well microtitre plate[23] and the CC_{50} values were determined. The biological activity results suggest that several of the compounds show good activity and low cytotoxicity, especially compounds **12i** and **12l** with MIC of 5.18 μM and 5.59 μM respectively (Table 3).

Docking study of compounds, **12a-l** shows that most active compound, **12i** tends to dock in a manner similar to bedaquiline and shows similar interaction with Glu-61 (Fig. 7). The least active compound **12g**, on the contrary docks and interacts in a dissimilar pattern (Fig. 8). A plot of log MIC versus dock score (Fig. 9) shows a correlation with $r^2 = 0.705$, suggesting the possible activity of arylquinoline derivatives as *Mtb*ATPase inhibitors.

The biological data of arylquinoline derivatives aids us to postulate a structure activity relationship (SAR). The ligands with conformationally restricted terminal amino group such as pyrrolidine (**12i** – **12l**), show better activity as compared to the flexible terminal amino group such as diethylamine (**12a** – **12d**). Also, morpholine, when used as the terminal amino group (**12e** – **12h**), possibly due to its bulkiness or due to presence of oxygen, does not allow the formation of H-bond between the amino terminal and Glu-61 as seen in docking, leading to decrease in activity. Furthermore, electronegative substitution at para position of phenyl ring increases the activity (**12d**, **12h**, **12l**), while electropositive substitution at para position of phenyl ring decreases the activity (**12c**, **12g**, **12k**).

In conclusion, a novel series of arylquinoline derivatives have been synthesized as potential anti-tuberculosis agents, by retaining the crucial pharmacophoric features of bedaquiline and maintaining a similar three dimensional geometry. The structural similarity of the molecules with bedaquiline and the observed correlation between in vitro and in silico results, suggests that the compounds may act by inhibiting *Mtb*ATPase. These results suggest that arylquinoline based compounds could serve as a promising scaffold for further tuberculosis drug development. Our efforts are now focused on exploring the mechanistic details of the molecules along with series expansion.

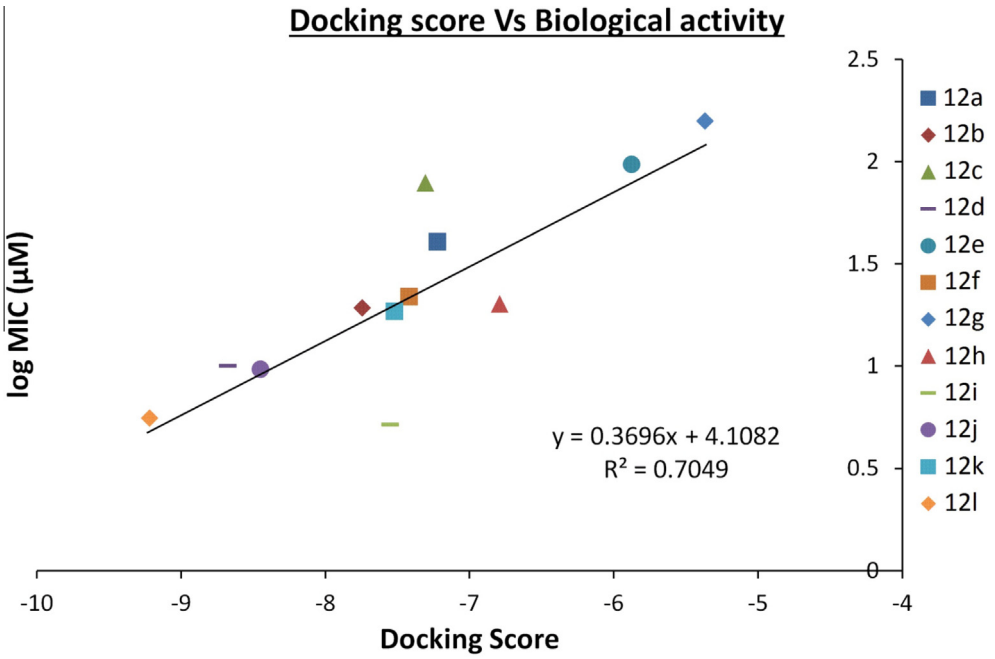

Figure 9. Linear relationship between in vitro and in silico results.

Acknowledgement

P.J. is thankful to University Grants Commission (UGC), India for financial support.

Supplementary data

Supplementary data associated with this article can be found, in the online version, at http://dx.doi.org/10.1016/j.bmcl.2013.09.027.

References and notes

1. World Health Organization *Global Tuberculosis Report 2012 (in IRIS)*; World Health Organization: Geneva, 2012.
2. Udwadia, Z. F.; Amale, R. A.; Ajbani, K. K.; Rodrigues, C. *Clin. Infect. Dis.* **2012**, *54*, 579.
3. Welsch, M. E.; Snyder, S. A.; Stockwell, B. R. *Curr. Opin. Chem. Biol.* **2010**, *14*, 347.
4. Upadhayaya, R. S.; Kulkarni, G. M.; Vasireddy, N. R.; Vandavasi, J. K.; Dixit, S. S.; Sharma, V.; Chattopadhyaya, J. *Bioorg. Med. Chem.* **2009**, *17*, 4681.
5. Andries, K.; Verhasselt, P.; Guillemont, J.; Gohlmann, H. W.; Neefs, J. M.; Winkler, H.; Van Gestel, J.; Timmerman, P.; Zhu, M.; Lee, E.; de Williams, P.; Chaffoy, D.; Huitric, E.; Hoffner, S.; Cambau, E.; Truffot-Pernot, C.; Lounis, N.; Jarlier, V. *Science* **2005**, *307*, 223.
6. Huitric, E.; Verhasselt, P.; Andries, K.; Hoffner, S. E. *Antimicrob. Agents Chemother.* **2007**, *51*, 4202.
7. Haagsma, A. C.; Abdillahi-Ibrahim, R.; Wagner, M. J.; Krab, K.; Vergauwen, K.; Guillemont, J.; Andries, K.; Lill, H.; Koul, A.; Bald, D. *Antimicrob. Agents Chemother.* **2009**, *53*, 1290.
8. Walsh, S. FDA approves first drug to treat multi-drug resistant tuberculosis. In *FDA Press Announcement*, 2012.
9. Sastry, G. M.; Dixon, S. L.; Sherman, W. *J. Chem. Info. Model.* **2011**, *51*, 2455.
10. Boyer, P. D. *Annu. Rev. Biochem.* **1997**, *66*, 717.
11. von Ballmoos, C.; Wiedenmann, A.; Dimroth, P. *Annu. Rev. Biochem.* **2009**, *78*, 649.
12. Yoshida, M.; Muneyuki, E.; Hisabori, T. *Nat. Rev. Mol. Cell Biol.* **2001**, *2*, 669.
13. Haagsma, A. C.; Podasca, I.; Koul, A.; Andries, K.; Guillemont, J.; Lill, H.; Bald, D. *PloS one* **2011**, *6*, e23575.
14. Rastogi, V. K.; Girvin, M. E. *Nature* **1999**, *402*, 263.
15. de Jonge, M. R.; Koymans, L. H.; Guillemont, J. E.; Koul, A.; Andries, K. *Proteins* **2007**, *67*, 971.
16. Maestro, Version 9.3; Schrödinger, LLC: New York, NY, 2012.
17. Qikprop, Version 3.5; Schrödinger, LLC: New York, NY, 2012.
18. Meth-Cohn, O.; Narine, B. *Tetrahedron Lett.* **1978**, *19*, 2045.
19. Vogel, A. I.; Tatchell, A. R.; Furnis, B. S.; Hannaford, A. J.; Smith, P. W. G. *Vogel's Textbook of Practical Organic Chemistry*, 5th ed.; Prentice Hall, 1996.
20. Bakalarz, A.; Heliński, J.; Krawiecka, B.; Michalski, J.; Potrzebowski, M. J. *Tetrahedron* **1999**, *55*, 12211.
21. Gaertner, V. R. *J. Org. Chem.* **1968**, *33*, 523.
22. Palomino, J. C.; Martin, A.; Camacho, M.; Guerra, H.; Swings, J.; Portaels, F. *Antimicrob. Agents Chemother.* **2002**, *46*, 2720.
23. Freshney, R. I. *Culture of Animal Cells: A Manual of Basic Technique and Specialized Applications*; Wiley-Blackwell: Hoboken, N.J., 2010.